



**QUEEN'S
UNIVERSITY
BELFAST**

Bayesian Analysis of ^{210}Pb Dating

Aquino Lopez, M., Blaauw, M., Christen, J. A., & Sanderson, N. K. (2018). Bayesian Analysis of ^{210}Pb Dating. *Journal of Agricultural, Biological, and Environmental Statistics*, 1-18. DOI: 10.1007/s13253-018-0328-7

Published in:

Journal of Agricultural, Biological, and Environmental Statistics

Document Version:

Publisher's PDF, also known as Version of record

Queen's University Belfast - Research Portal:

[Link to publication record in Queen's University Belfast Research Portal](#)

Publisher rights

Copyright 2018 the authors.

This is an open access article published under a Creative Commons Attribution License (<https://creativecommons.org/licenses/by/4.0/>), which permits unrestricted use, distribution and reproduction in any medium, provided the author and source are cited.

General rights

Copyright for the publications made accessible via the Queen's University Belfast Research Portal is retained by the author(s) and / or other copyright owners and it is a condition of accessing these publications that users recognise and abide by the legal requirements associated with these rights.

Take down policy

The Research Portal is Queen's institutional repository that provides access to Queen's research output. Every effort has been made to ensure that content in the Research Portal does not infringe any person's rights, or applicable UK laws. If you discover content in the Research Portal that you believe breaches copyright or violates any law, please contact openaccess@qub.ac.uk.

Bayesian Analysis of ^{210}Pb Dating

Marco A. AQUINO-LÓPEZ , Maarten BLAAUW ,
J. Andrés CHRISTEN , and Nicole K. SANDERSON

In studies of environmental change of the past few centuries, ^{210}Pb dating is often used to obtain chronologies for sedimentary sequences. One of the most commonly used approaches to estimate the age of material at different depths in a sequence is to assume a constant rate of supply (CRS) or influx of ‘unsupported’ ^{210}Pb from the atmosphere, together with a constant or varying amount of ‘supported’ ^{210}Pb . Current ^{210}Pb dating models do not use a proper statistical framework and provide poor estimates of the uncertainties. Here, we develop a new model for ^{210}Pb dating, where ages and values of supported and unsupported ^{210}Pb form part of the parameters. We apply our model to a case study from Canada as well as to some simulated examples. Our model can extend beyond the current CRS approach, deal with asymmetric errors and mix ^{210}Pb with other types of dating, thus obtaining more robust, realistic and statistically better defined age estimates.

Key Words: Chronology; Constant rate of supply; Lead dating; MCMC; Sediment core.

1. INTRODUCTION

^{210}Pb (lead-210) is a radioactive isotope which forms part of the ^{238}U (uranium) decay series. ^{238}U (solid) is contained within most rocks, and over time it decays into ^{226}Ra (radium, solid), which then decays into ^{222}Rn (radon, gas). Because ^{222}Rn is a gas, a proportion escapes to the atmosphere where it decays into ^{210}Pb (solid) which is in turn transported to the earth’s surface by precipitation. ^{210}Pb deposited this way is labelled ‘unsupported’ or excess ^{210}Pb (P^U). On the other hand, ^{222}Rn decaying in situ becomes what is labelled as ‘supported’ ^{210}Pb (P^S). By assuming a constant supply of unsupported ^{210}Pb (Appleby and Oldfield 1978; Robbins 1978) and distinguishing between supported and unsupported ^{210}Pb , one can determine the age of sediment. Given that the half-life of ^{210}Pb is 22.3

Marco A. Aquino-López (✉) and Maarten Blaauw, School of Natural and Built Environment, Queen’s University Belfast, Belfast BT7-1NN, UK (E-mail: maquinolopez01@qub.ac.uk) (E-mail: maarten.blaauw@qub.ac.uk).
J. Andrés Christen, Centro de Investigación en Matemáticas (CIMAT), Jalisco s/n, Valenciana, 36023 Guanajuato, GT, Mexico (E-mail: jac@ciimat.mx). Nicole K. Sanderson, College of Life and Environmental Sciences, University of Exeter, Exeter EX4-4QJ, UK (E-mail: N.K.Sanderson@exeter.ac.uk).

© 2018 The Author(s)

Journal of Agricultural, Biological, and Environmental Statistics
<https://doi.org/10.1007/s13253-018-0328-7>

years, the dating limit for this isotope is 150–200 years, depending on the conditions and equipment used to measure it.

The current dating approach used throughout the ^{210}Pb community is called the constant rate of supply (CRS) model (Appleby and Oldfield 1978; Robbins 1978; see Appendix A), and it is frequently used in recent past climate studies, sometimes in combination with radiocarbon dates (such as Munoz et al. 2018). Unfortunately, the CRS model was not developed within a satisfactory statistical framework. This resulted in a series of uncertainty approximations (Binford 1990; Appleby 2001; Sanchez-Cabeza et al. 2014), which use error propagation and assume normality around the estimated ages. Since the original method uses the radioactive decay equation ($N(t) = N_0 e^{-\lambda t}$, where $N(t)$ is the quantity of a radioactive element left in the sample at age t , N_0 is the initial quantity, and λ is the element's radioactive decay constant) to infer the ages, it results in a logarithmic approximation to a series of dates. This logarithmic approximation heavily restricts the age-depth model.

In this work, we introduce both a new treatment of ^{210}Pb data and a new dating model created within a formal statistical framework, with the objective of providing more reliable measures of uncertainty as well as more accurate dates from ^{210}Pb measurements.

The paper is organized as follows: Sect. 2 introduces a statistical treatment of ^{210}Pb data, as well as the necessary tools for a Bayesian analysis of these data (prior distributions and likelihood), Sect. 3 shows the implementation of this approach, Sect. 4 compares the CRS and our model using real data, Sect. 5 introduces a mechanism to simulate ^{210}Pb data (using the constant rate of supply assumption) which allows us to test the model in different scenarios. Lastly, details about the CRS model and the modelling of supported and unsupported ^{210}Pb can be found in Appendices A and B, respectively.

2. A STATISTICAL APPROACH TO ^{210}Pb DATING

Let the concentration of ^{210}Pb in a sample taken from a core section $(x_i - \delta, x_i)$ be a random variable denoted p_i . The core section depth x_i and the sample's thickness δ are typically both measured in cm. Since each concentration p_i is measured independently from others, it is safe to assume that each p_i is conditionally independent and is normally distributed with mean, the unknown total concentration P_i^T , and variance as reported by the laboratory, namely

$$p_i | P_i^T \sim \mathcal{N}\left(P_i^T, \sigma_i^2\right). \quad (1)$$

Each sample p_i contains both supported (P^S) and unsupported (P^U) ^{210}Pb . ^{210}Pb from these two sources is indistinguishable, which means that certain assumptions or measurements have to be made to find the supported ^{210}Pb (see Appendix B). In this case, the supported ^{210}Pb is assumed to be in equilibrium throughout the core, which means that it remains constant through all depths. If necessary, a supported ^{210}Pb per sample can easily be included by letting P_i^S be different for each sample i . It is important to note that this will greatly increase the number of parameters and should only be used in cases where the hypothesis of a constant supported concentration has been shown to be unreasonable. If a

constant supported ^{210}Pb is a valid assumption, then we can use $P_i^T = P^S + P_i^U$, otherwise $P_i^T = P_i^S + P_i^U$; the only difference being that P^S is global parameter, whereas P_i^S only affects the sample i .

Now, assuming a constant rate of supply (Appleby and Oldfield 1978; Robbins 1978, see Appendix B for details), the unsupported activity in sample i can be obtained as follows:

$$A_i^U = \int_{x_i-\delta}^{x_i} \rho_i(z) P_i^U(z) dz = \int_{t(x_i-\delta)}^{t(x_i)} \Phi e^{-\lambda\tau} d\tau = \frac{\Phi}{\lambda} \left(e^{-\lambda t(x_i-\delta)} - e^{-\lambda t(x_i)} \right), \quad (2)$$

where ρ_i is the density of sample i , Φ is the supply of ^{210}Pb , and $t(x)$ is the sample's age (years since the material was deposited) at depth x . On the other hand, assuming the supported ^{210}Pb is constant in the core, the supported activity of sample i is

$$A_i^S = \int_{x_i-\delta}^{x_i} \rho(z) P^S(z) dz = P^S \rho_i. \quad (3)$$

Now, we can define $y_i = p_i \rho_i$

$$y_i | P^S, \Phi, \bar{t} \sim \mathcal{N} \left(A_i^S + \frac{\Phi}{\lambda} \left(e^{-\lambda t(x_i-\delta)} - e^{-\lambda t(x_i)} \right), (\sigma_i \rho_i)^2 \right). \quad (4)$$

It is important to note that the activity at each sample contains not only information regarding its age, but also of the supported ^{210}Pb (P^S) and of the initial supply of unsupported ^{210}Pb (Φ) throughout the core.

2.1. PRIOR DISTRIBUTIONS

To implement a Bayesian approach, prior distributions for each parameter have to be defined. Appleby (2001) suggested that the supply of unsupported ^{210}Pb has a global mean of $50 \frac{\text{Bq}}{\text{m}^2\text{yr}}$ (becquerel, Bq, is the International System of Units unit for radioactivity, $\frac{\text{Bq}}{\text{m}^2\text{yr}}$ is the unit of measure of yearly supply of ^{210}Pb to the sediment, $\frac{\text{Bq}}{\text{m}^2}$ is the activity of ^{210}Pb factored by density of the sediment, and $\frac{\text{Bq}}{\text{kg}}$ is the raw concentration of ^{210}Pb). In our research, we have encountered case studies ranging from $20 \frac{\text{Bq}}{\text{m}^2\text{yr}}$ up to $180 \frac{\text{Bq}}{\text{m}^2\text{yr}}$. Using this information, we fix a prior distribution for Φ . Since Φ is always positive, a gamma distribution is a good default choice and we define $\Phi \sim \text{Gamma}(a_\Phi, b_\Phi)$; using Appleby's global mean we can define $E(\Phi) = 50 \frac{\text{Bq}}{\text{m}^2\text{yr}}$. Additionally, using a shape parameter $a_\Phi = 2$ allows Φ to be flexible enough to incorporate the information we have available while allowing for more extreme values.

On the other hand, since supported ^{210}Pb (P^S) varies much from site to site, data regarding this variable are necessary ($y_1^S, y_2^S, \dots, y_{n_s}^S$). These data can come from two different sources (see Appendix B); ^{226}Ra estimates or ^{210}Pb measurements from depths where unsupported ^{210}Pb is no longer detected. A prior distribution for P^S associated with these data is necessary. Little is known regarding this parameter prior to obtaining the data. We have seen cores ranging from nearly 0 Bq/kg up to almost 50 Bq/kg of supported ^{210}Pb .

With this information, a gamma distribution with a mean of 20 Bq/kg and shape parameter $a_S = 2$ would allow the data to contribute largely to the posterior value of P^S . Lastly, in order to define a prior distribution for the ages, an age-depth function has to be defined.

2.2. AGE-DEPTH FUNCTION

Since sediment cores can extend back thousands of years, ^{210}Pb is not the only technique used to date them. ^{14}C (radiocarbon) is a common way to obtain age estimates for organic material, ranging back up to 50,000 years of age. The radiocarbon community has built sophisticated chronology models, which rely on equally sophisticated age-depth functions, with the objective of properly quantifying the uncertainty of the resulting chronology. Since we want our approach to have the flexibility to incorporate other dating information such as radiocarbon, we decided to incorporate a well-established age-depth function.

Bacon (Blaauw and Christen 2011) is one of the most popular Bayesian chronology models for ^{14}C dating. By using the same structure, age-depth models based on multiple isotopes could be obtained. With this in mind, we decided to base our age-depth model on *Bacon*. Now, we discuss the general construction of the *Bacon* age-depth function (see Blaauw and Christen 2011, for details). This age-depth function is linear over sections of equal length, causing depths to be divided into sections of equal length $c_0 < c_1 < \dots < c_K$ noting that in this case $c_0 = 0$. Within these sections, linear accumulation is assumed, so for section $c_i < d < c_{i+1}$ the model can be expressed as

$$G(d, m) = \sum_{j=1}^i m_j \Delta c + m_{i+1} (d - c_i), \quad (5)$$

where $m = (m_1, m_2, \dots, m_k)$ are the slopes of each linear interpolation, and $\Delta c = c_i - c_{i+1}$ is the length of each section.

With this structure, a gamma autoregressive model is proposed for the accumulation rate of each section, $m_j = \omega m_{j+1} + (1 - \omega)\alpha_j$ where $\alpha_j \sim \text{Gamma}(a_\alpha, b_\alpha)$ and $\omega \in [0, 1]$ is a memory parameter which is distributed as $\omega \sim \text{Beta}(a_\omega, b_\omega)$.

Using the above age-depth function and (4), the model's log-likelihood takes the form

$$\ell(\bar{y}, \bar{y}^S \mid m, \omega, \Phi, P^S) \propto - \sum_{i=1}^n \frac{\left(y_i - \left(A_i^S + \frac{\Phi}{\lambda} \left(e^{-\lambda G(x_{i-1}, m)} - e^{-\lambda G(x_i, m)} \right) \right) \right)^2}{2\sigma_i^2} - \sum_{j=1}^{n_S} \frac{(y_j^S - P^S)}{2\sigma_j^2}. \quad (6)$$

Using the prior distributions previously mentioned, a posterior distribution $f(m, \omega, \Phi, P^S \mid \bar{y}, \bar{y}^S)$ is defined, from which we may obtain Monte Carlo samples using MCMC. To allow for faster convergence of the MCMC, a limit to the chronology is considered. This chronology limit is inspired by the ^{210}Pb dating horizon, which is the age at which ^{210}Pb samples lack any measurable unsupported ^{210}Pb .

2.3. CHRONOLOGY LIMIT

The ^{210}Pb dating horizon was described by Appleby (1998) to be 100–150 years, based on the available knowledge and measurement techniques at the time, but the dating horizon of a given core is affected by different factors. The first of them is the equipment used to measure the samples. If certain equipment has higher precision than another, it will be able to distinguish unsupported from supported ^{210}Pb down to deeper samples and thus provide ages further back in time. The other factor that impacts the dating horizon is the quantity of initial unsupported ^{210}Pb , which is directly affected by the rate of supply (Φ). When there is a larger initial unsupported ^{210}Pb , it will take longer for the unsupported ^{210}Pb in a sample to become indistinguishable from the supported ^{210}Pb , again providing ages further back in time.

We therefore decided to set a dynamic chronology limit for our method. This limit (t_l) will be determined by two factors—the rate of supply of ^{210}Pb to the site (Φ) and the error related to the equipment used to measure the samples. For example, let us assume that the equipment used to calculate the concentration of ^{210}Pb in a sample has a minimum error of $0.01 \frac{\text{Bq}}{\text{kg}}$. Now, assuming that the sample comes from a bog with a peat density ranging between 0.05 and $0.2 \frac{\text{g}}{\text{cm}^3}$ (Chambers et al. 2011), then once the unsupported activity in a sample reaches $A_l \simeq 0.1 \frac{\text{Bq}}{\text{m}^2}$, it becomes indistinguishable from the supported activity. This information could help us to calculate the dynamic age limit. By using Eq. (2), we have

$$A_l = \int_{t_l}^{t_l+1} \Phi e^{-\lambda\tau} d\tau = \Phi e^{-\lambda t_l} \frac{1 - e^{-\lambda}}{\lambda},$$

where A_l is the minimum distinguishable unsupported activity in a sample related to the equipment's error, Φ is the supply of ^{210}Pb to the site, and $\lambda = 0.03114$ is the decay constant, and considering that $\frac{1 - e^{-\lambda}}{\lambda} = 0.98459$, then

$$t_l = \frac{1}{\lambda} \log \left(\frac{0.98459\Phi}{A_l} \right) \simeq \frac{1}{\lambda} \log \left(\frac{\Phi}{A_l} \right). \quad (7)$$

It is important to note that this limit depends on the error of the equipment and on the origin of the samples, which are factors known prior to obtaining the data. Moreover, Φ is a parameter of the model. This will allow the model to limit the chronology given Φ .

3. IMPLEMENTATION AND MCMC

Blaauw and Christen (2011) propose the use of a self-adjusting MCMC algorithm, known as t-walk (Christen and Fox 2010), which will facilitate the use of these techniques to non-statisticians (i.e. most users of ^{210}Pb dating). The t-walk algorithm requires two initial points for all parameters (Φ , P^S , w , α) and the negative of the log posterior function which is called the energy function,

$$U(\Phi, P^S, w, \alpha | \bar{y}, \bar{y}^S) = -\log f(\Phi, P^S, w, \alpha | \bar{y}, \bar{y}^S). \quad (8)$$

Table 1. HP1C data set presenting the necessary information to replicate the results from the CRS model as well as from our approach.

Depth cm	^{210}Pb Bq/kg	$\sigma(^{210}\text{Pb})$ $\sigma(\text{Bq/kg})$	Density (ρ) g/cm^2	Depth cm	^{210}Pb Bq/kg	$\sigma(^{210}\text{Pb})$ $\sigma(\text{Bq/kg})$	Density (ρ) g/cm^2
1	371.730	11.900	0.045	18	279.320	11.140	0.045
2	456.390	15.080	0.047	19	243.820	9.940	0.045
3	454.240	17.110	0.051	20	246.750	9.170	0.054
4	449.640	14.430	0.049	21	351.680	13.100	0.086
5	479.040	16.440	0.049	22	281.280	11.380	0.089
6	490.970	16.750	0.051	23	235.300	12.720	0.099
7	482.120	16.780	0.050	24	192.820	7.240	0.085
8	486.880	15.200	0.047	25	94.280	4.740	0.066
9	431.580	14.830	0.048	26	50.550	3.410	0.060
10	422.750	16.210	0.049	27	36.080	2.260	0.062
11	315.310	13.030	0.052	28	28.710	2.100	0.055
12	349.770	15.220	0.047	29	24.680	1.760	0.059
13	301.740	13.450	0.051	35	11.040	1.270	0.356
14	284.410	10.020	0.050	40	6.240	1.010	0.414
15	280.580	11.620	0.053	45	10.150	1.310	0.347
16	250.170	9.760	0.048	50	7.960	1.600	0.352
17	267.740	12.950	0.048				

We wrote a program (in Python 2.7) to implement this approach and to sample from the posterior distribution. We call our program *Plum*. *Plum* has been tested on peat and lake sediment cores, as well as on simulated data, delivering a reasonable MCMC, with no need to further tune its parameters. Examples of these results can be seen in Sects. 4 and 5. The consistency of these results, with minimal user input, shows how the t-walk (Christen and Fox 2010) was a suitable choice for this implementation.

4. MODEL COMPARISON

To implement our approach in a real case study, data obtained from a site in Havre-St-Pierre, Quebec, Canada will be used. The core (HP1C) was obtained in July 2012 and was analysed using alpha spectrometry at Exeter University, UK. HP1C's data are presented in Table 1. *Plum* was set to use the bottom-most 4 samples to estimate the supported activity for this core, and the rest of the data to establish the chronology. Figure 1 also shows a comparison with results using the CRS model (Appleby 2001). From this comparison, we can observe that both models agree with each other down to a depth of 25 cm, at which point the CRS model continues at a similar slope unlike our approach which provides younger estimates. This uninterrupted growth of the CRS model can be explained by its logarithmic approximation to the age function, which invariably tends to infinity as unsupported ^{210}Pb reaches 0. Even with these discrepancies, both models have overlapping confidence intervals, with our approach providing a more precise chronology in the topmost part and a more conservative estimate for the deepest part of the core.

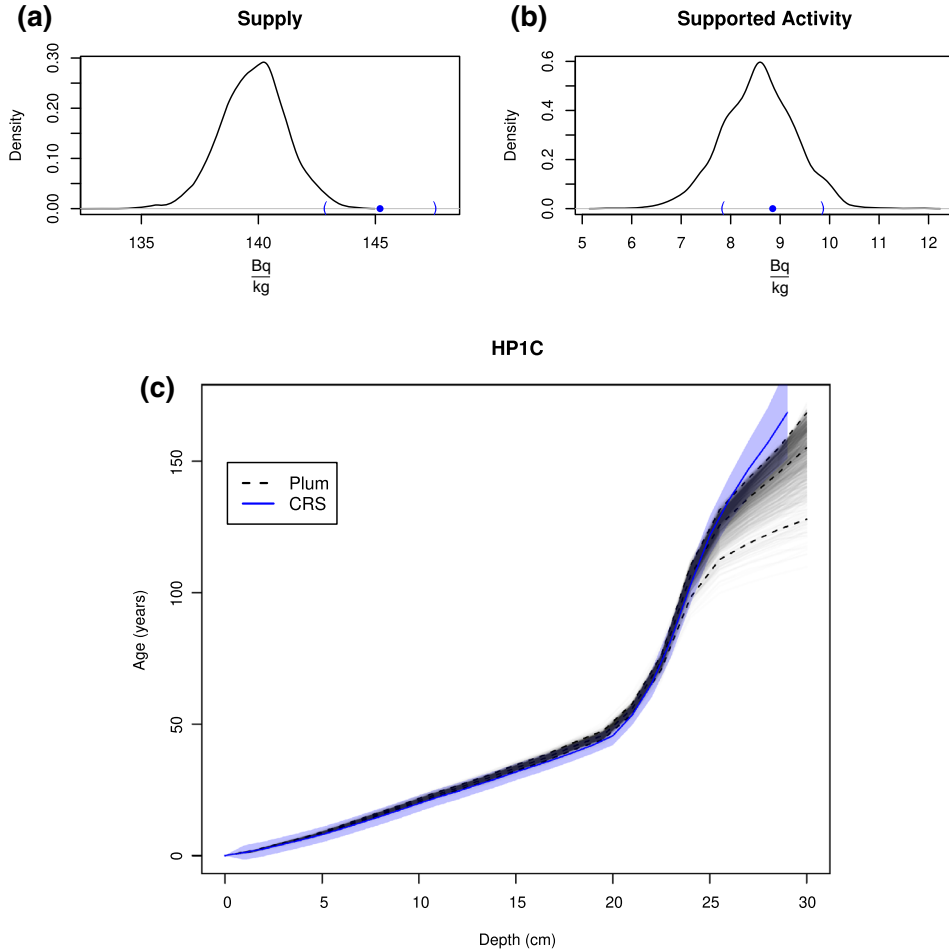


Figure 1. **c** Comparison between the CRS (Appleby 2001) and our model using data from HP1C. Blue curve and shadow indicate CRS mean and its corresponding 95% range. Dashed black curves indicate mean and 95% confidence interval for our model. Grey lines are simulations from *Plum*. The top curves represent estimates of the supply of unsupported ^{210}Pb (Φ) **(a)** and supported ^{210}Pb (P^S) **(b)** using the CRS model (blue; dot shows the mean, parentheses show the standard deviation) and *Plum* (black curve) (Color figure online).

This example shows the potential of our approach in a ‘well-behaved’ real-world case study. We still need to observe the precision and accuracy of our approach when confronted with more challenging data sets, such as those that do not reach the background and/or have missing data. For this purpose, we created several simulated scenarios where we know the ‘true’ chronology and can observe how our approach behaves in more challenging circumstances.

5. SIMULATED EXAMPLE

To obtain simulated data, a constant supply of ^{210}Pb was defined as $\Phi = 150 \frac{\text{Bq}}{\text{kg}}$, and by using the constant rate of supply assumption from Appleby and Oldfield (1978) and Robbins

Table 2. Simulated data set presenting the necessary information to replicate *Plum*'s results as well as those of the CRS model (Appleby 2001).

Depth cm	^{210}Pb (P^T) Bq/kg	$\sigma(^{210}\text{Pb})$ $\sigma(\text{Bq/kg})$	Density (ρ) g/cm ²	Depth cm	^{210}Pb (P^T) Bq/kg	$\sigma(^{210}\text{Pb})$ $\sigma(\text{Bq/kg})$	Density (ρ) g/cm ²
1	102.897	10	0.145	16	80.845	7	0.150
2	180.761	9	0.145	17	64.024	7	0.151
3	220.507	9	0.145	18	48.792	7	0.151
4	268.669	9	0.145	19	54.076	7	0.152
5	285.026	9	0.146	20	37.109	7	0.152
6	311.949	9	0.146	21	36.640	7	0.153
7	298.226	9	0.146	22	28.602	7	0.153
8	302.736	9	0.146	23	22.180	6	0.154
9	262.598	8	0.147	24	29.342	6	0.154
10	251.080	8	0.147	25	28.723	6	0.154
11	221.818	8	0.148	26	26.123	6	0.154
12	199.937	8	0.148	27	17.803	6	0.155
13	161.476	8	0.149	28	23.349	6	0.155
14	132.268	8	0.149	29	13.607	6	0.155
15	112.069	8	0.150	30	16.825	5	0.155

(1978) we have $P_0(x)r(x) = 150$. At this point, we can define $\rho(x)$ to obtain $r(x)$ and by defining the age function as $t(x) = x^2/3 + x/2$, we obtain :

$$\rho(x) = 1.5 - .05 \cos\left(\frac{x}{30\pi}\right) \quad (9)$$

$$P_0(x) = \frac{150\left(\frac{2x}{3} + \frac{1}{2}\right)}{\rho(x)}. \quad (10)$$

Using these functions, simulated samples at any given depth can be obtained by integrating each function between the top and bottom depths of the sample. Lastly, to simulate supported ^{210}Pb , a constant value was added to the simulations such that $P_i = P^S(b - a) + \int_a^b P^U(x)dx$, where a and b are the top and bottom depths of the sample. For this simulation, we set the supported ^{210}Pb to $P^S = 20$. To replicate the measurement errors related to the concentration of ^{210}Pb , white noise was added such that $P_i + \epsilon$ where P_i is the concentration found in sample i and $\epsilon \sim \mathcal{N}(0, \sigma_i)$. This exercise provided us with the simulated data set in Table 2. We use this simulated data set to test the precision and accuracy of our approach in various circumstances. For this purpose, the last three sample points were designated as estimates of the supported ^{210}Pb .

The first scenario was for ^{210}Pb age-depth models where every core section is measured, from the surface to where background is reached. In this scenario, both approaches should obtain reasonable results, thus providing the complete information about the decay of unsupported ^{210}Pb . This scenario can be simulated using the complete data set from Table 2. Figure 2 shows the comparison between the chronology obtained by our model and that of the CRS (Appleby 2001) alongside the real age function, and how both models include the true chronology in their 95% intervals. By applying our approach to this scenario, we obtained a very accurate chronology by taking the mean of the MCMC simulations. This

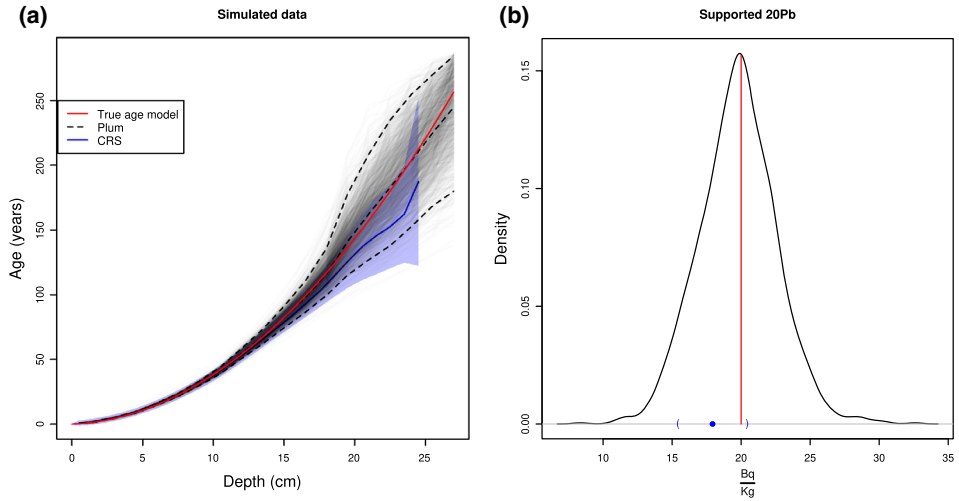


Figure 2. **a** Comparison between the CRS (Appleby 2001) and our model using simulated data. Blue curve and shadow indicate CRS mean and its corresponding 95% range. Dashed black curves indicate mean and 95% confidence interval for our model. Grey lines are simulations from *Plum*. Red curve is the true age-depth model. **b** [cut] Estimates of the supported ^{210}Pb (P^S) using the CRS model (blue; dot shows the mean, parentheses show the standard deviation) and *Plum* (black curve). True supported ^{210}Pb (P^S) is marked by a red line (Color figure online).

shows, unsurprisingly, that our model behaves quite well in the best-case scenario. On the other hand, the CRS model provides a shorter chronology, since some samples had to be discarded (the bottom-most samples is always discarded; see Appendix A). This is a direct result from the logarithmic approximation mentioned in Sect. 4. In this particular case, the two bottom-most P_i^U had to be discarded because the deepest P_i^U sample (depth 27 cm in Table 2) was smaller than the estimated supported activity. The CRS estimates younger ages at the bottom, which can be a result of the underestimated supported ^{210}Pb as can be observed in Fig. 2. Another feature of the CRS worth mentioning is the rapid growth of the chronology in the bottom sample. As previously mentioned, this rapid increase can be attributed to the logarithmic approximation the CRS uses.

The following scenarios deal with the behaviour of our model in circumstances where there is no complete dating information. Even if we were to attempt to use the CRS model to provide age estimate in these scenarios, it would do this by interpolating and extrapolating in the sections where there is missing data. Applying the CRS model to these simulations would require us to take several additional heuristic decisions with large potential impacts on the chronology (e.g. exponential or linear extrapolation beyond and/or between the dated levels, see Sanchez-Cabeza and Ruiz-Fernández 2012). Such comparisons lie outside the scope of the present work, but will be explored in a future study, and consequently for the next examples we only study the performance of the *Plum* chronology.

Sometimes, researchers do not have the funds to obtain a full, continuously measured data set for the chronology that they want to build. When this is the case, only certain strategically placed samples are measured. To simulate this scenario, only the data at odd depths were used to obtain the chronology. Figure 3a shows the results from this experiment.

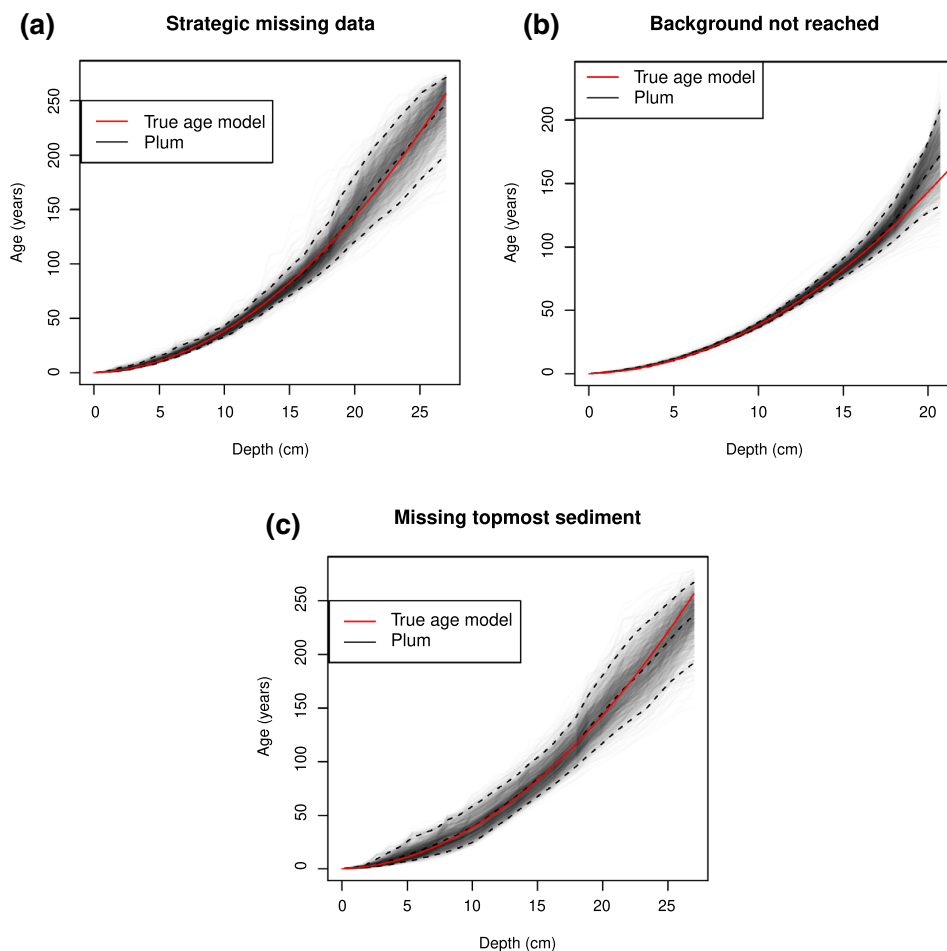


Figure 3. Bayesian analysis of simulated ^{210}Pb data using odd depths in the top-left, using samples with depths 1–20 in the top-right and using the samples with depths 1 and 11–27 in the bottom-centre. The red line represents the true age-depth function, grey lines are simulations from *Plum*, and dashed lines represent the 95% interval and mean (Color figure online).

The accuracy of the model did not change as it still gives an accurate estimate of the true age model, and the precision was not greatly affected even though only half of the available data were used to calculate this chronology.

A common problem in ^{210}Pb dating is not reaching background. To observe the behaviour of our model, the bottom-most seven data points were removed where background was not reached. Figure 3 presents the resulting chronology compared to the true age function. The chronology is accurate down to a depth of 16 cm, from which point it provides older estimates. On the other hand, the model's confidence ranges enclose the true chronology at all times even for the older ages.

The last scenario to which our approach was tested is missing the topmost sediment. For this example, the data points with a depth of 2 to 10 cm depth were removed. Figure 3c

BAYESIAN ANALYSIS OF ^{210}Pb DATING

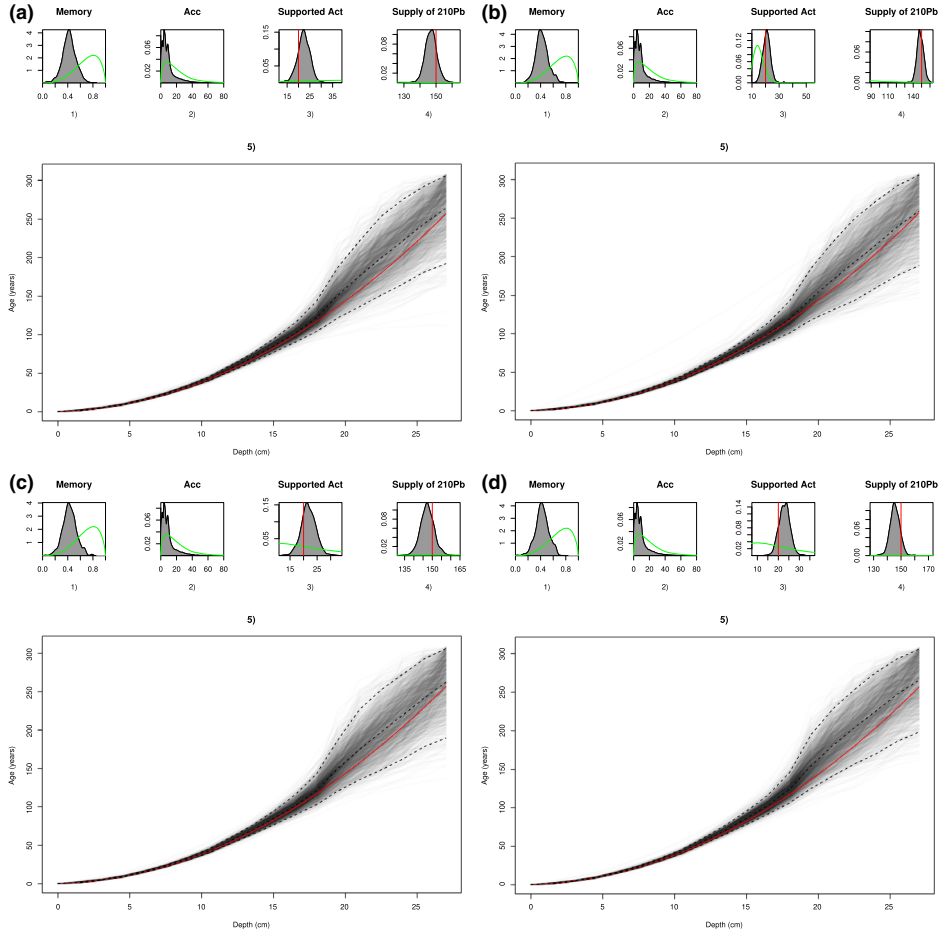


Figure 4. Bayesian analysis of simulated ^{210}Pb data using different prior distributions: small panels (1) show the prior (in green) and posterior (in grey) distributions for the memory ω (labels 1), (2) accumulation rate α , (3) supported ^{210}Pb (P^S) (red vertical line represents the true value of the parameter), (4) the supply of ^{210}Pb (Φ) and (5) the resulting chronology (in red the true age function and black dashed lines represent the 95% interval and mean). Figures in section **a** represent the results from using $E(P^S) = 100$ and $a_\Phi = 2$, section **b** $E(P^S) = 15$ and $a_\Phi = 15$, **c** $E(\Phi) = 500$ and $a_\Phi = 2$, and **d** $E(\Phi) = 50$ and $a_\Phi = 15$ (Color figure online).

shows the results of this experiment. Even with a third of consecutive missing data, the model is able to accurately reconstruct the true age function.

Another use of the simulated data is to observe the behaviour of the posterior distributions when different prior information is used. This can be an indicator of how robust the method is to changes in the prior information. Blaauw and Christen (2011)'s supporting material shows the results of changing the parameters related to the chronology (w , α). We conducted the same experiment concerning these two parameters, changing α 's shape parameter from 3 to 200 and $E(\alpha)$ to 30, and ω 's strength $a_\omega + b_\omega = 5$ and its $E(\omega) = .5$, with similar results (results not shown). On the other hand, our approach to ^{210}Pb dating also estimates variables regarding the behaviour of ^{210}Pb (supported ^{210}Pb P^S and supply of ^{210}Pb Φ). To

observe how sensitive our model is to the prior distribution of these two parameters, we ran *Plum* using four different settings (see Fig. 4). The first of these changes is altering $E(\Phi)$ to 500 and leaving the shape parameter $a_\Phi = 2$. Even with this significant change to $E(\Phi)$, Φ 's posterior distribution manages to estimate the true value and none of the other parameters are affected. The second experiment on parameter Φ is to change the shape parameter a_Φ to 15 and leave $E(\Phi) = 50$. Using this modified prior distribution, once again no significant changes in any of the posterior distributions can be observed. Further, the prior distribution of P^S is first modified to have $E(P^S) = 100$ and $a_{ps} = 2$, and then, $E(P^S) = 15$ and $a_{ps} = 15$ again with no significant impact to the posterior distribution.

With these results, we can presume that modifying the prior distributions for P^S or Φ within reasonable limits does not significantly affect the posterior distributions or the resulting chronology. The only scenario which significantly impacted our approach was missing data which affected the precision, as was to be expected, but had hardly on accuracy.

6. DISCUSSION

Our approach to ^{210}Pb dating creates a structure in which the data are the result of a physical model, which allows us to have a more realistic measurement of the chronology uncertainty. Therefore, the main disadvantage of our approach comes from the intensive computing power that is needed, common to most modern Bayesian approaches. In this case, a run of *Plum* for a core of 30 cm with a section width of 1.5 cm takes about 40 to 50 minutes. This could be improved by writing *Plum* in a faster computer language such as C++.

Another potential disadvantage of our approach comes from the need to educate non-statisticians on how to interpret the resulting chronology as well as the posterior distributions of variables such as the supported concentration and flux of ^{210}Pb . Also, since a Bayesian approach makes use of prior information, the results can potentially be affected by unrealistic changes to its prior distributions as shown by Blaauw and Christen (2011)'s supporting material. If reasonable changes to these prior distribution are made, our approach remains robust as shown in Sect. 5. On the other hand, the advantage comes from a more realistic measure of uncertainties, since the ages are parameters which are inferred in the process. Moreover, dealing with missing data, which is a common problem when dealing with ^{210}Pb dating, becomes easier because our model does not need the whole core to be measured to obtain accurate results. Also, since the CRS model relies on a ratio, that approach requires removal of the bottom-most measurement. Since our methodology does not rely on a ratio, all the samples provide information to the chronology, making longer chronologies possible.

Given the integration of the supported ^{210}Pb we have into our model, a posterior distribution of this variable can be obtained, as well as for ages at any given depth (not just those with ^{210}Pb measurements) and the supply of ^{210}Pb to the site. Figure 1 shows the posterior distributions of the supported ^{210}Pb and the supply of unsupported ^{210}Pb . These posterior distributions provide realistic estimates of the uncertainty of these variables, which may be used for other studies where the main focus is not the chronology but other aspects of the site.

Another advantage of this methodology is the fact that since the model operates within a Bayesian framework, incorporating extra information is possible without having to ‘double-model’ by using previously modelled ages within an age-depth model. This information could come in the form of other radiometric ages, such as radiocarbon determinations. Since measurements of radiocarbon and ^{210}Pb , given the age, are independent, the overall likelihood would consist of two parts: the likelihood from ^{210}Pb and from ^{14}C . Therefore,

$$\mathcal{L}(\Theta) = \mathcal{L}_{210\text{Pb}}(\Theta) \mathcal{L}_{14\text{C}}(\Theta). \quad (11)$$

Considering that the only link between both data is $t(x)$, by using the same age-depth function such as that from Eq. (5), a chronology with both sources of data is possible. This becomes very important since the calibration curve (Reimer et al. 2013), which is used to correct the radiocarbon ages, is nonlinear for the most recent few centuries, causing problems with interpreting radiocarbon ages. This period is partly covered by ^{210}Pb . By combining these two methodologies, more robust chronologies could be obtained for this important period in human and environmental history.

Open Access This article is distributed under the terms of the Creative Commons Attribution 4.0 International License (<http://creativecommons.org/licenses/by/4.0/>), which permits unrestricted use, distribution, and reproduction in any medium, provided you give appropriate credit to the original author(s) and the source, provide a link to the Creative Commons license, and indicate if changes were made.

[Received October 2017. Accepted May 2018.]

A. THE CONSTANT RATE OF SUPPLY (CRS)

The constant rate of supply (CRS) (Robbins 1978; Goldberg 1963; Appleby and Oldfield 1978) model is the most commonly used ^{210}Pb dating model. It uses the constant rate of supply assumption presented in Sect. B.2, and the following equations to obtain a chronology:

$$A^U(x) = \int_x^\infty \rho(z) P^U(z) dz, \quad (A.1)$$

$$A^U(0) = \int_0^\infty \rho(z) P^U(z) dz, \quad (A.2)$$

$$t(x) = \frac{1}{\lambda} \ln \left(\frac{A^U(0)}{A^U(x)} \right), \quad (A.3)$$

where $A^U(x)$ is the remaining unsupported activity below x and $A^U(0)$ is the unsupported activity in the whole core. The CRS model can be summarized by Eq. (A.3), and from its term $A^U(0)$ one can deduce that this model depends strongly on measuring activity throughout the whole core. The effect of wrongly estimating this variable is described in Appleby (1998). If the activity cannot be measured throughout the entire core, interpolation is suggested (Appleby 2001). Moreover, if the bottom sample has not reached background, and thus still contains unsupported ^{210}Pb , extrapolation is suggested.

Because the CRS model is based only on the unsupported activity, realistic estimates of supported ^{210}Pb are necessary in order to obtain reliable estimates of the unsupported ^{210}Pb . Depending on the equipment used to obtain the ^{210}Pb concentrations, and on the model used to distinguish supported from unsupported ^{210}Pb , this could be problematic. Wrongly estimating this variable will directly impact the estimate of $A(0)$, as this would increase/decrease the amount of unsupported activity introduced into the model, resulting in a wrong estimate of $A(0)$, in turn affecting the resulting chronology.

To show the results of the current approach, data from HPIC were used. As mentioned in Sect. B.1, alpha spectrometry does not provide estimates of ^{226}Ra as is the case for beta spectrometry, but instead, compared to the latter, it can measure far smaller quantities of ^{210}Pb . To date this core, the CRS model was calculated using the recommendations in Appleby (2001).

One of the first steps to apply the CRS model is to identify the supported ^{210}Pb . For this purpose, the last 4 samples were averaged to obtain an estimate of $8.11 \frac{\text{Bq}}{\text{kg}}$ and a standard deviation of 1.01 for the supported activity. This value was subtracted from the total ^{210}Pb for each sample, to obtain estimates of unsupported activity. Following Appleby (2001), one can obtain the dating shown in Fig. 1. This methodology requires very strong assumptions regarding independence, given the fact that it uses accumulated activity as the primary tool for inference.

B. MODELLING OF ^{210}PB DATA

Within sediment ^{210}Pb is naturally formed from two sources—from surrounding sediment and rocks containing ^{238}U (supported), and from the atmosphere through ^{220}Rn (unsupported). Since supported and unsupported ^{210}Pb are indistinguishable from each other, in order to model both sources, we have to make assumptions depending on the measurement techniques used. Measurements of ^{210}Pb can be obtained by alpha or gamma spectrometry. The latter technique provides estimates of other isotopes such as ^{226}Ra , which can be used as a proxy of the supported ^{210}Pb in a sample (Krishnaswamy et al. 1971).

B.1 SUPPORTED ^{210}PB

If gamma spectrometry is used, supported ^{210}Pb can be assumed to be equal to the concentrations of ^{226}Ra . When the sediments are analysed using alpha spectrometry, ^{226}Ra measurements are not available and estimates of the supported activity can only be obtained by analysing sediment which reached background (samples which no longer contain unsupported ^{210}Pb). Therefore, when alpha spectrometry is used, a constant supported ^{210}Pb is assumed. These two different ways of inferring the supported activity can be formalized by the following equations:

$$P_i^T = P_i^S + P_i^U, \quad (\text{A.4})$$

$$P_i^T = P^S + P_i^U, \quad (\text{A.5})$$

where P_i^T is the total ^{210}Pb , P_i^U is the unsupported ^{210}Pb , P_i^S is the supported ^{210}Pb in sample i , and P^S is the constant supported ^{210}Pb when constant levels of ^{210}Pb are assumed. Depending on the site and availability of measuring techniques, one of these equations can be used to differentiate supported from unsupported ^{210}Pb .

B.2 UNSUPPORTED ^{210}Pb

In order to model the unsupported ^{210}Pb , some assumptions have to be made regarding the precipitation of this material from the atmosphere. A reasonable assumption for this phenomenon is the constant flux or rate of supply (Appleby and Oldfield 1978), which implies that for fixed periods of time the same amount of ^{210}Pb is supplied to the site.

Following Appleby and Oldfield (1978), the assumption of a constant rate of supply implies that the initial concentration of ^{210}Pb at depth x (which is linked to age by a function $t(x)$), $P_0^U(t(x))$, weighed by the dry mass sedimentation rate $r(t(x))$, is constant throughout the core:

$$P_0^U(t(x))r(t(x)) = \Phi, \quad (\text{A.6})$$

where Φ is a constant. The dry sedimentation rate is the speed at which the sediment accumulates, weighed by the sediment's density at such depth, i.e.

$$r(t(x)) = \rho(x) \frac{dx(t)}{dt}, \quad (\text{A.7})$$

where $\rho(x)$ is defined as the density of the sediment at depth x and $\frac{dx(t)}{dt}$ is the rate at which the core accumulates with respect to time. Considering that the relationship between depth and time is expressed by the function $t(x)$, then $x(t)$ is the inverse function of time, and since $t(x)$ is a one-to-one function

$$r(t(x)) = \rho(x) \left[\frac{dt(x)}{dx} \right]^{-1}. \quad (\text{A.8})$$

Since ^{210}Pb is a radioactive isotope, it follows from the radioactive decay equation that

$$P^U(x) = P_0^U(t(x))e^{-\lambda t(x)}, \quad (\text{A.9})$$

where $P^U(x)$ is the concentration of unsupported ^{210}Pb found at depth x and λ is the ^{210}Pb half-life. Using Eqs. (A.6), (A.8) and (A.9), the following relationship is obtained:

$$\rho(x)P^U(x) = \frac{dt(x)}{dx} \Phi e^{-\lambda t(x)}. \quad (\text{A.10})$$

Considering that ^{210}Pb is measured over a slice or section of the sediment, this relationship has to be integrated over such section to be related to the corresponding measurement, that

is,

$$A_{(a,b)}^U = \int_a^b \rho(z) P^U(z) dz \quad (\text{A.11})$$

$$= \int_a^b \Phi e^{-\lambda t(z)} \frac{dt(z)}{dz} dz$$

$$= \int_{t(a)}^{t(b)} \Phi e^{-\lambda y} dy, \quad (\text{A.12})$$

where (a, b) are the lower and upper depths of the sample, respectively, and $A_{(a,b)}^U$ is the activity in section (a, b) . Equation (A.12) provides a link between the age-depth function $t(x)$ and the unsupported activity in a given section. This is the primary tool to construct an age-depth model based on a constant rate of supply.

REFERENCES

- Appleby, P. G. (1998), "Dating recent sediments by Pb-210: Problems and solutions," *Proc. 2nd NKS/EKO-1 Seminar, Helsinki, 2-4 April 1997, STUK, Helsinki*, pp. 7–24.
- Appleby, P. G. (2001), "Chronostratigraphic Techniques in Recent Sediments," *Tracking Environmental Change Using Lake Sediments: Basin Analysis, Coring, and Chronological Techniques*, pp. "171–203".
- Appleby, P., and Oldfield, F. (1978), "The calculation of lead-210 dates assuming a constant rate of supply of unsupported 210Pb to the sediment," *Catena*, 5(1), 1–8.
- Binford, M. W. (1990), "Calculation and uncertainty analysis of ^{210}Pb dates for PIRLA project lake sediment cores," *Journal of Paleolimnology*, 3, 253–267.
- Blaauw, M., and Christen, J. A. (2011), "Flexible paleoclimate age-depth models using an autoregressive gamma process," *Bayesian Analysis*, 6(3), 457–474.
- Chambers, F. M., Beilman, D. W., and Yu, Z. (2011), "Methods for determining peat humification and for quantifying peat bulk density, organic matter and carbon content for palaeostudies of climate and peatland carbon dynamics," *Mires and Peat*, 7, 1–10. URL: <http://mires-and-peat.net/pages/volumes/map07/map0707.php>
- Christen, J. A., and Fox, C. (2010), "A general purpose sampling algorithm for continuous distributions (the t-walk)," *Bayesian Anal.*, 5(2), 263–281. URL: <https://doi.org/10.1214/10-BA60>
- Goldberg, E. D. (1963), "Geochronology with Pb-210," *Radioactive Dating*, pp. 121–131.
- Krishnaswamy, S., Lal, D., Martin, J., and Meybeck, M. (1971), "Geochronology of lake sediments," *Earth and Planetary Science Letters*, 11(1-5), 407–414.
- Munoz, S. E., Giosan, L., Therrell, M. D., Remo, J. W. F., Shen, Z., Sullivan, R. M., Wiman, C., O'Donnell, M., and Donnelly, J. P. (2018), "Climatic control of Mississippi River flood hazard amplified by river engineering," *Nature*, 556, 95 EP–. URL: <https://doi.org/10.1038/nature26145>
- Reimer, P. J., Bard, E., Bayliss, A., Beck, J. W., Blackwell, P. G., Bronk, M., Grootes, P. M., Guilderson, T. P., Hafflidason, H., Hajdas, Hatte, C., Heaton, T. J., Hoffman, D. L., Hogg, A. G., Hughhen, K. A., Kaiser, J. F., Kromer, B., Manning, S. W., Niu, M., Reimer, R. W., Richards, D. A., Scott, E. M., Southon, J. R., Staff, R. A., Turney, C. S. M., and van der Plicht, J. (2013), "IntCal 13 and Marine 13 radiocarbon age calibration curves 050,000 years cal BP," *Radiocarbon*, 55, 1869–1887.
- Robbins, J. (1978), "Geochemical and geophysical applications of radioactive lead," *The biogeochemistry of lead in the environment*, pp. 285–393.
- Sanchez-Cabeza, J. A., and Ruiz-Fernández, A. C. (2012), " ^{210}Pb sediment radiochronology: An integrated formulation and classification of dating models," *Geochimica et Cosmochimica Acta*, 82, 183–200.

BAYESIAN ANALYSIS OF ^{210}Pb DATING

Sanchez-Cabeza, J. A., Ruiz-Fernández, A. C., Ontiveros-Cuadras, J. F., Pérez Bernal, L. H., and Olid, C. (2014), "Monte Carlo uncertainty calculation of ^{210}Pb chronologies and accumulation rates of sediments and peat bogs," *Quaternary Geochronology*, 23, 80–93.